

# "Sub-Microsecond Pulse Heating Measurements of High Temperature Electrical Resistivity of the 3d-Transition Metals Fe, Co, and Ni"

U. Seydel and W. Fücke

Institut für Experimentalphysik der Universität Kiel

(Z. Naturforsch. **32 a**, 994–1002 [1977]; received May 27, 1977)

The exploding wire technique is suitable for the determination of the electrical resistivity of metals in a wide temperature range provided that the heating of the wire material in the liquid phase occurs fast enough to avoid changes in the wire geometry due to surface tension. It is also an appropriate method for measuring latent heats of fusion especially for refractory metals.

The electrical resistivity  $\varrho$  and the enthalpy  $H$  are derived from time-resolved measurements of current and voltage of exploding wires, which are part of a fast RCL-discharge circuit. The time interval for heating the wire from room temperature to the normal boiling point is typically  $1\ \mu\text{sec}$ . Because of the short times involved interactions with the surrounding medium are negligible. The time resolution of the system is better than  $8\ \text{nsec}$  and the estimated error of measured resistivity and enthalpy above temperatures of  $1000\ \text{K}$  is less than  $4\%$ .

For Fe, Co, and Ni the  $\varrho(H)$ -dependence up to the normal boiling point and the therefrom derived  $\varrho(T)$ -dependence are reported and compared with steady-state experiments.

## 1. Introduction

The measurement of specific heat, electrical resistivity and many other thermophysical properties at very high temperatures (above  $2000\ \text{K}$ ) involves some severe problems. The usually applied steady-state or quasi steady-state methods result in a relatively long exposure of the specimen to high temperatures and with that to thermal and chemical reactions with the surrounding medium.

A very promising approach to avoid these problems was attempted by Cezairliyan and co-workers<sup>1</sup>, who developed a subsecond pulse heating technique for the dynamic measurement of heat capacity, electrical resistivity, hemispherical total emittance, and normal spectral emittance of electrical conductors at high temperatures. Because the geometry of the specimen — a tube with a wall thickness of about  $0.5\ \text{mm}$  — is destroyed during melting, this method is restricted to temperatures up to the beginning of melting.

The destruction of the geometry of the specimen in the liquid phase can be avoided by still faster heating using the exploding wire technique<sup>2–6</sup>. Of course, with very fast resistive heating new problems arise as for example the possibility of non-uniform current distribution due to transient effects, which would lead to an inhomogeneous temperature distribution over the cross section of the cylindrical

sample. In addition, the fast heating may possibly prevent the sample from uniform expansion to a stable equilibrium volume. Furthermore, magneto-hydrodynamic instabilities — the so-called striations — may be generated and cause longitudinal inhomogeneities. The experimental or theoretical consideration of these effects for the determination of high-temperature thermophysical properties of metals will be discussed below.

## 2. Experimental Set-up

The rapid pulse heating of the samples is achieved by a RCL-discharge. The experimental system consists of a fast RCL-pulsing circuit, fast measuring circuits for the time-resolved measurement of current and voltage, and of optical control systems for the checking of the macroscopic state of the specimen.

A diagram of the discharge circuit including the measuring systems is presented in Figure 1. The complete system is similar to that described earlier<sup>7</sup> but is complemented by a fast current viewing resistor (shunt). The mainly coaxial RCL-discharge circuit is emphasized by broader lines. It consists of a capacitor-bank with a capacitance of  $5.1\ \mu\text{F}$ , which can be charged up to  $35\ \text{kV}$ . From the short-circuit ringing period of  $6.4\ \mu\text{sec}$  a total inductivity of  $200\ \text{nH}$  is deduced. The circuit resistance comes out to  $20\ \text{m}\Omega$ .

For the measurement of the dynamic electrical quantities three measuring heads are installed: a coaxial ohmic voltage divider, a coaxial current viewing resistor (CVR), and an induction-coil,

Reprint requests to Dr. U. Seydel, Institut für Experimentalphysik der Christian-Albrechts-Universität, Olshausenstraße 40–60, D-2300 Kiel 1.



Dieses Werk wurde im Jahr 2013 vom Verlag Zeitschrift für Naturforschung in Zusammenarbeit mit der Max-Planck-Gesellschaft zur Förderung der Wissenschaften e.V. digitalisiert und unter folgender Lizenz veröffentlicht: Creative Commons Namensnennung-Keine Bearbeitung 3.0 Deutschland Lizenz.

Zum 01.01.2015 ist eine Anpassung der Lizenzbedingungen (Entfall der Creative Commons Lizenzbedingung „Keine Bearbeitung“) beabsichtigt, um eine Nachnutzung auch im Rahmen zukünftiger wissenschaftlicher Nutzungsformen zu ermöglichen.

This work has been digitalized and published in 2013 by Verlag Zeitschrift für Naturforschung in cooperation with the Max Planck Society for the Advancement of Science under a Creative Commons Attribution-NoDerivs 3.0 Germany License.

On 01.01.2015 it is planned to change the License Conditions (the removal of the Creative Commons License condition "no derivative works"). This is to allow reuse in the area of future scientific usage.

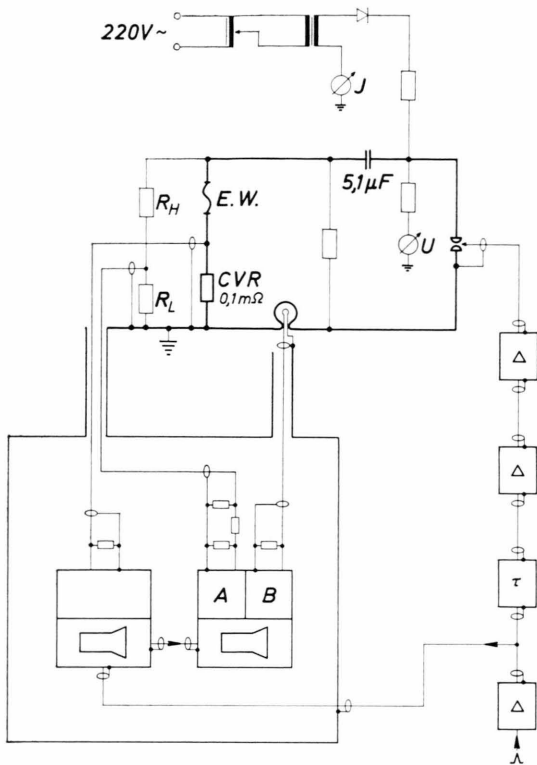


Fig. 1. Schematic diagram of the RCL-discharge circuit.  $R_H$ ,  $R_L$ : voltage divider; E.W.: sample (exploding wire); CVR: current viewing resistor.

which is placed in an  $\Omega$ -shaped part of the current transmission line. In connection with 150 MHz-oscilloscopes (Tektronix type 7704) all measuring systems have rise-times less than 8 nsec.

A thorough grounding and multiplex screening of the entire measuring system guarantee low hum and noise.

The optical control system includes a high-speed rotating-mirror camera with a time resolution better than 8 nsec<sup>7</sup> and an image-converter camera, used at exposure times of 10 nsec. Both systems operate time correlated with the electrical measurements. The application of these optical systems allows checking the complete suppression of peripheral arcs and the expansion of the wire material with rising temperature as well.

### 3. Experimental Performance and Evaluation

The CVR and the induction-coil offer two independent methods for measuring the current:

1. The voltage drop across the CVR is exactly proportional to the current and can therefore be

converted into current units if the resistance of the CVR is known.

2. The  $dI/dt$ -signal from the induction-coil is transformed into a signal proportional to the current by means of a RC-integrator with a proper time-constant. The absolute calibration is obtained from the ringing period and the logarithmic decrement of a short-circuit oscillation.

This calibration procedure was applied to two current oscillograms obtained from the same discharge by the two different methods and the discrepancy for the first current maximum was only 8‰. The calibration of the CVR lay with 6‰ deviation within the tolerance of 1‰ for the resistance given by the producer. Thus both current measuring methods are likewise reliable, at least for the time intervals of interest. The determination of the voltage across the specimen is somewhat more difficult. Because of the unavoidable self-inductance of the discharge gap the signal from the voltage divider includes an ohmic part  $R \cdot I$  as well as an inductive part  $d/dt (L \cdot I)$ . For the determination of the time dependence of the electrical resistivity or the energy only the ohmic term is to be considered. Assuming that no change in the inductivity of the discharge gap occurs during the time interval to be investigated, i. e. the expansion of the wire material can be neglected, the inductive term is proportional to  $dI/dt$ . The elimination of this term can therefore be performed by subtracting from the voltage divider signal a suitably amplified  $dI/dt$ -signal obtained from the induction-coil. The amplification factor follows from the condition that at  $t=0$  no voltage step should occur. This compensation procedure has to be repeated each time wires with different geometries are used.

From the current and voltage oscillograms the current density  $i(t) = I(t)/A$ , the electrical resistivity  $\varrho(t) = U(t)A/I(t)l$ , and the enthalpy  $H = H(T) - H(298 \text{ K}) = \int_{t_0}^t [U(t)I(t)/AD] dt$  are computed, where  $A$ ,  $l$ ,  $D$  stand for the cross section, the length, and the density of the wire, respectively, all taken at room temperature.

The enthalpy is defined at constant pressure. Because of the RCL-characteristic of the discharge, however, we have to consider a strongly varying current in the initial stage of the heating process and therefore a pinch-pressure varying with time and increasing towards the wire center.

This pressure is generated by the magnetic field and therefore the work performed by it has not to be considered in the total energy balance because the inductive component of the enthalpy is ruled out by the compensation method applied.

The maximum current and with that the maximum pressure occurs before melting as can be seen from Figures 3 a–c. This pressure amounts to  $p = 3800$  atm in the wire center or, averaged over the radius, to  $\bar{p} = 1900$  atm for a maximum current of approximately 13.8 kA (Co). In the solid state the error resulting from the application of the enthalpy using constants given at normal pressure is negligible.

The error from the pressure-dependence of the resistivity can also be neglected<sup>8</sup>.

A transformation of  $H$  into temperature is performed on the basis of values tabulated by Kelley<sup>9</sup>.

For the computation of the resistivity from voltage and current the geometry of the specimen at room temperature is taken as a basis. Therefore, the change in volume with rising temperature has to be taken into account in a correction. Figure 2 shows photographs of Ni-wires taken with an image-converter camera at a twelvefold magnification. The upper picture is a zero-photograph and the middle one is taken at the instant marked in the voltage oscillogram. Assuming that the expansion in the solid state occurs in both the radial and the axial direction and during melting and in the liquid state only in the radial direction<sup>3,5</sup> the correction factor for the resistivity can be deduced from these pictures. Within the margin of error these values agree with data for the change in density  $-dD/dT$  in the liquid state given by Steinberg<sup>10</sup>.

The shock waves in Fig. 2 are generated at the melting transition when the wire expands in a very short time (20–80 nsec) for about 2–6% of its volume depending on the material. The energy dissipated in these shock waves, however, has only to be taken into account for those experiments performed at high current densities (above  $2 \cdot 10^7$  Acm<sup>-2</sup> at the melting transition).

The change in wire cross-section causes a change in the inductivity of the coaxial discharge gap. But at the same time transient skin effect causes a change of current distribution and with that of the inner inductivity in the outer conductor. We think that these two effects will nearly cancel out each other and no additional voltage drop will occur. Calcula-

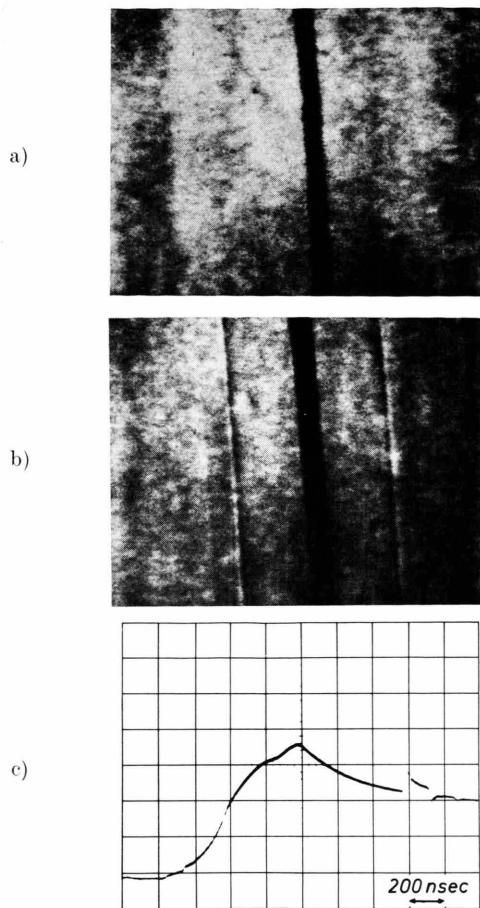


Fig. 2. Image-converter photograph of the sample before (top) and during the heating process (middle) at the instant marked in the voltage oscillogram.

tions for the confirmation of this presumption are in preparation. The influence of transient skin effect in the inner conductor (the wire) on the electrical measurements should be negligible because of the relatively high resistivity of the investigated elements Fe, Co, and Ni at room temperature<sup>11</sup>. A more detailed discussion of this effect is given in an earlier publication<sup>12</sup>.

#### 4. Measurements and Results

Measurements of the temperature dependence of the electrical resistivity at very high temperatures have been carried out for the 3d-transition elements Fe, Co, and Ni.

The experimental parameters have been the same for all three elements: voltage  $U_0 = 8$  kV, wire length  $l = 4.75$  cm, wire diameter  $d = 0.025$  cm. The surrounding medium has been water.

The chemical purity has been 99.99% for all three elements. The impurities as taken from chemical analysis by the manufacturer are listed below in Table 1.

Impurity	Composition ppm		
	Fe	Co	Ni
Ag	1	2	1
Al	2	1	1
Bi	—	<1	—
Ca	3	1	1
Cr	1	<1	<1
Cu	2	3	3
Fe		7	15
Mg	2	1	<1
Mn	1	<1	<1
Ni	1	2	
Si	3	5	2
Sn	—	1	<1

Table 1.  
Chemical impurities in Fe,  
Co, and Ni specimens.

In the Figs. 3 a – c current and voltage oscillograms for Fe, Co, and Ni up to the normal boiling point and beyond are presented. The small negative dips are time marks for the time correlation of current and voltage.

Figures 4 a – c show the  $\varrho(H)$ -dependence for the three elements under investigation as computed from  $I(t)$  and  $U(t)$  considering (full line) and not considering (dashed line) the change in density. The curves are averages over six single experiments in each case.

For all three elements the position of the Curie-point and the beginning and the completion of melting can be deduced from the  $\varrho(H)$ -plots and are marked with a, b, and c, respectively. These fixed points are very well suited for comparisons with steady-state measurements.

In Figs. 5 a – c the  $\varrho(T)$ -dependence is plotted up to the temperature of normal boiling. In all cases the own measurements are compared with steady-state values as far as these are available.

In Table 2 the measured latent heats of fusion for Fe, Co, and Ni as derived from own measurements are listed and compared with values given by Kelley<sup>9</sup>.

Table 2. Heat of fusion.

Element	Heat of fusion $\Delta H/\text{Jg}^{-1}$	
	own measurement	Kelley <sup>9</sup>
Fe	$275.0 \pm 12.2$	275.0
Co	$300.7 \pm 18.2$	291.1
Ni	$322.0 \pm 18.0$	300.1

Table 3 gives the values for the resistance temperature coefficient in the liquid phase between the melting temperature  $T_M$  and the normal boiling temperature  $T_B$ . The values for  $T_M$  and  $T_B$  are borrowed from<sup>13</sup>.

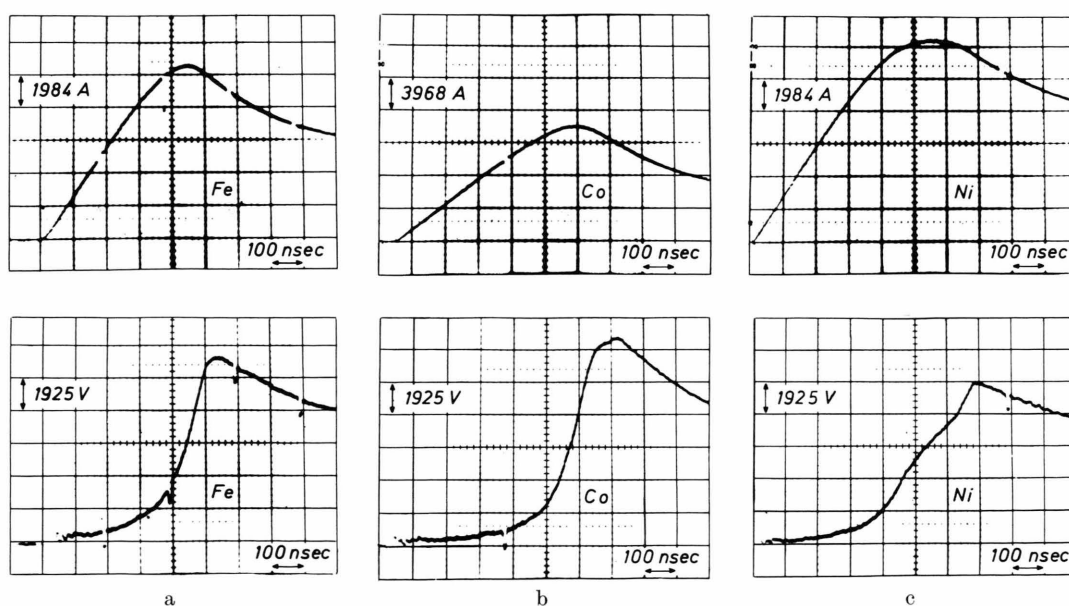


Fig. 3. Current and voltage oscillograms of a) Fe-, b) Co-, and c) Ni-wires exploded in water.

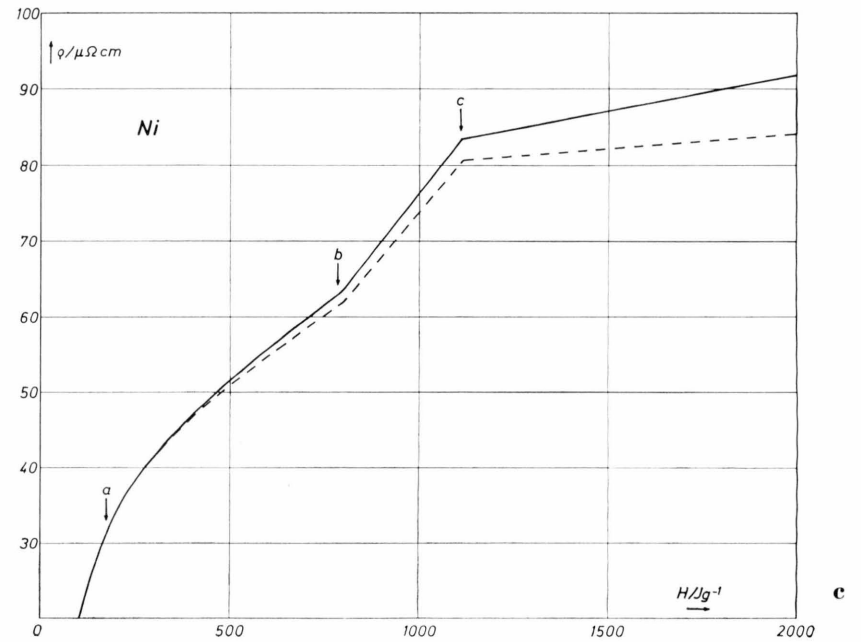
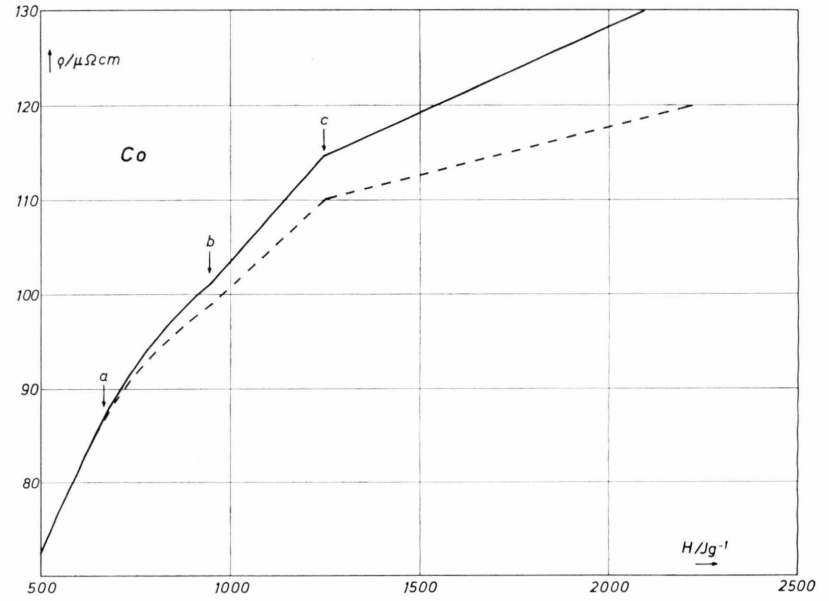
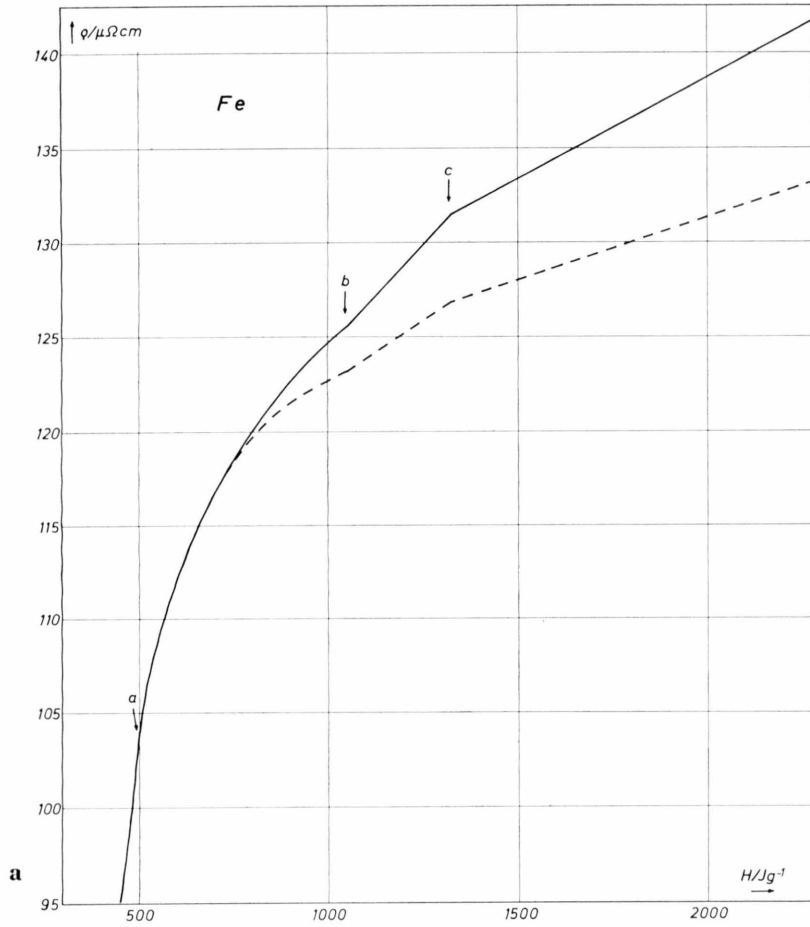


Fig. 4.  $\rho(H)$ -diagrams for a) Fe, b) Co, and c) Ni considering (full line) and not considering (dashed line) the change in density.

Element	$\varrho_T = \varrho_{T_M} [1 + \alpha(T - T_M)]$	$T_M \leq T \leq T_B$
Fe	$\varrho_T = 131.5 [1 + 7.07 \cdot 10^{-5} (T - 1809)]$	$1809 \leq T \leq 3148$
Co	$\varrho_T = 114.7 [1 + 9.89 \cdot 10^{-5} (T - 1768)]$	$1768 \leq T \leq 3174$
Ni	$\varrho_T = 83.5 [1 + 7.87 \cdot 10^{-5} (T - 1725)]$	$1725 \leq T \leq 3160$

Table 3. Resistance temperature coefficient in the liquid phase ( $\varrho$  in  $\mu\Omega\text{cm}$ ).

$T_M$  = melting temperature,  $T_B$  = boiling temperature.

### 5. Estimate of Errors

The systematic errors in the directly measured quantities current and voltage are hardly to be specified. They base on the calibration of the measuring heads, which is better than 1% in any case. The error in voltage measurement is enhanced by a time dependent part, which results mainly from a defective compensation of the inductive component. It decreases in the course of the heating process because of a decreasing  $dI/dt$ .

The statistical error for all three elements came out to less than 1% in the derived quantities  $\varrho$  and  $H$ .

Additional systematic errors may result from the data used for the computation of the changing wire geometry with rising temperature and for the transformation of the enthalpy into temperature.

A total error cannot be stated but from the very satisfying agreement between our results and those from steady-state methods can be estimated not to exceed a few percent in the liquid phase.

The relatively large statistical errors in the heats of fusion (Table 2) arise from the fact that each of them is a difference of two high enthalpy values with large absolute statistical errors.

### 6. Discussion and Conclusions

As can be inferred from Fig. 5 a – c for all three elements the  $\varrho(T)$ -behavior of the own measurements in the liquid phase shows a slower rise with temperature than that of the comparable steady-state measurements made by Güntherodt et al.<sup>14</sup> and by Regel and Mokrovsky<sup>15</sup>. It should be noted that

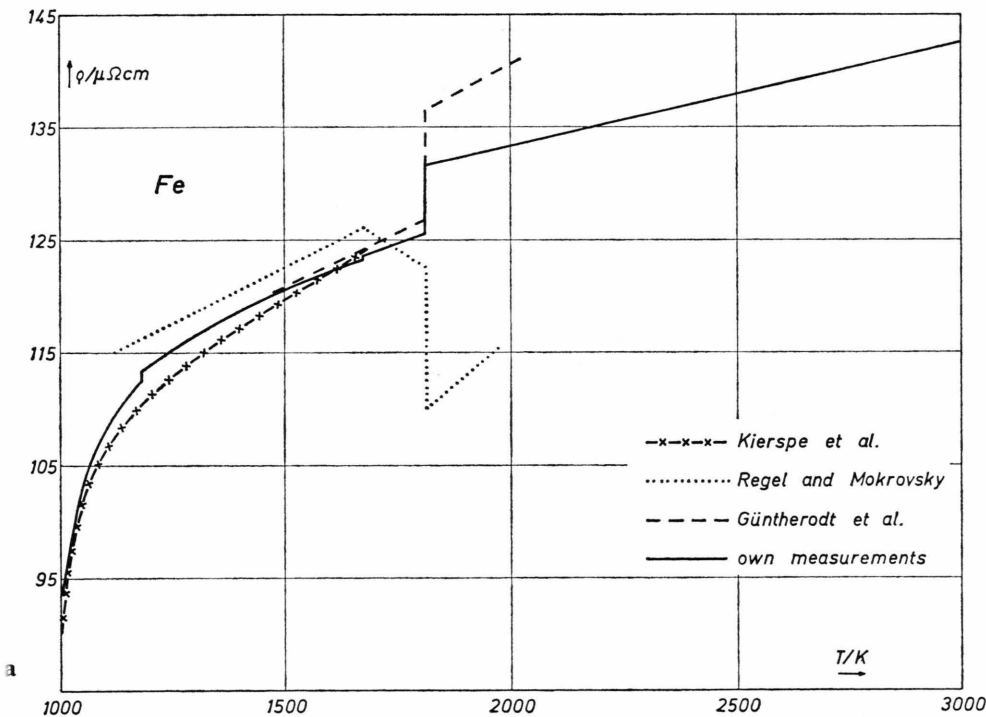
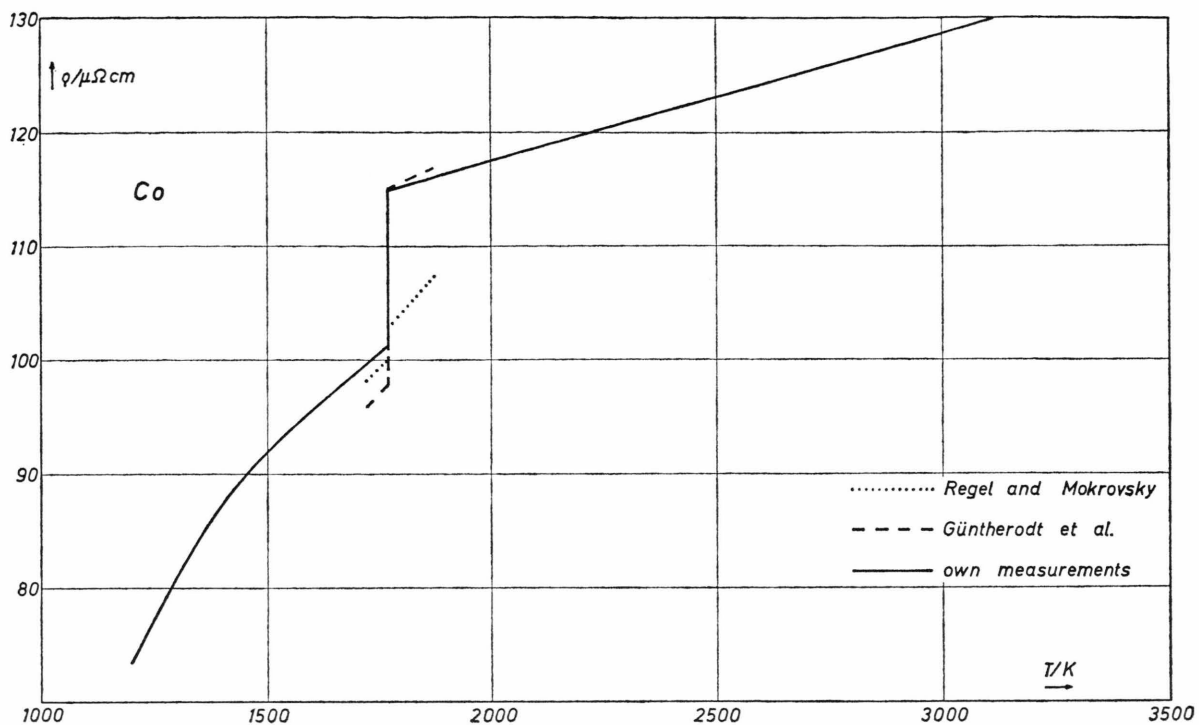
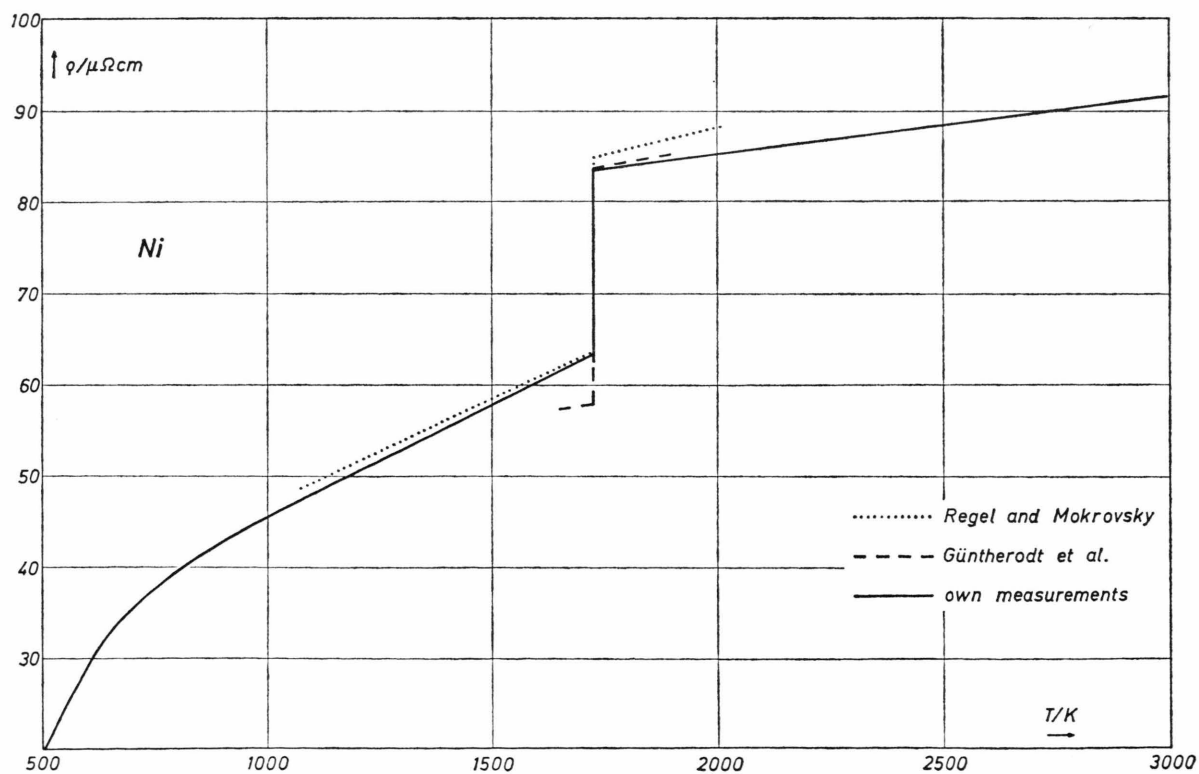


Fig. 5.  $\varrho(T)$ -diagrams for a) Fe, b) Co, and c) Ni.





b



c

the Regel and Mokrovsky measurements lie back more than twenty years. At least in the case of Fe they seem to be incorrect in the neighborhood of the melting transition.

The deviating  $\varrho(T)$ -behavior of our measurements in the liquid phase may – at least in part – be explained by the not fully cleared expansion behavior of the liquid metal subjected to a very fast ohmic heating process. The  $\varrho(H)$ -diagrams (Fig. 4 a – c), not corrected for changing density (dashed lines), do show only a more or less weak dependency of resistivity on rising enthalpy in the liquid phase. This behavior is most obvious for Fe and Ni. Here the value of the resistivity is mainly affected by the thermal expansion factor in the liquid phase. A similar observation has also been reported by Martynyuk et al.<sup>5</sup> over a wide temperature range for Zr, Hf, Mo, and Nb. These authors give two possible explanations for this effect: (1) The scattering cross-section for conduction electrons does not change as a function of  $T$  in the liquid phase, and  $\varrho$  is governed solely by the number of atoms per unit volume; (2) the scattering cross-section varies as a function of  $T$ , so that there should be a change in  $\varrho$ , but some other process, e. g., a change in the concentration of conduction electrons occurs simultaneously and acts to offset this change in the scattering cross-section.

Because the  $\varrho(T)$ -behavior of many d-transition metals depends critically on the volume changes in the liquid phase it is very important not only to get reliable data on the expansion behavior of the liquid metal but also to prevent the specimen from changes in geometry due to MHD-instabilities or surface tension. Savvatimskii<sup>6</sup> pointed out the possibility that deviations in data obtained from differently rapid processes may result from changes in shape in the slower ones. On the other hand Siebke<sup>16</sup> could establish that MHD-instabilities can be avoided most successfully by very fast heating. Furthermore, the image-converter photograph (Fig. 2) taken at a time beyond the investigated interval does not give any evidence for the existence of striations.

The capability of the described method may be demonstrated best at the  $\varrho(T)$ -diagram of Fe (Fig. 5 a), where the  $\beta$ - $\gamma$ - and the  $\gamma$ - $\delta$ -phase transitions are clearly to be located. The  $\varrho$ -value at the  $\gamma$ - $\delta$ -transition agrees very well with values given by Kierspe et al.<sup>17</sup> and recently by Cezairliyan and McClure<sup>18</sup>. The decrease in resistivity between the

$\gamma$ - $\delta$ -transition and the melting point as well as during melting reported by Regel and Mokrovsky does not seem to fit the true conditions. The agreement, however, between our results and those of Kierspe et al. in the solid state is very satisfying. The relatively small ratio of the resistivities in the liquid state  $\varrho_l$  and in the solid state  $\varrho_s$  at the melting point of  $(\varrho_l/\varrho_s)_{\text{Fe}} = 1.05 \pm 0.02$  found by us is not fully understood, yet we think it may in part be explained by oxidation of the samples and in part by incorrect values for the volume change.

A comparison of the Ni-data reported earlier<sup>12</sup> with the latest values confirms the assumption that the too high  $\varrho_s$ - and  $\varrho_l$ -values at the melting transition in<sup>12</sup> may be explained by the relatively high impurity of the wire material (1%). The ratio  $(\varrho_l/\varrho_s)_{\text{Ni}}$  is found to be  $1.31 \pm 0.02$  for pure Ni (99.99%).

Our  $\varrho(T)$ -data obtained for Co are also in good agreement with the comparable steady-state values<sup>14, 15</sup> close to the melting transition except with the values for  $\varrho$  in the liquid phase given by Regel and Mokrovsky. The ratio of the resistivities  $\varrho_l$  and  $\varrho_s$  is found to be  $(\varrho_l/\varrho_s)_{\text{Co}} = 1.13 \pm 0.02$ . For all three elements the experimentally determined ratio  $(\varrho_l/\varrho_s)$  is considerably lower than the value calculated on the basis of the Mott-formula  $(\varrho_l/\varrho_s) = \exp \{80 A/T_M\}$  ( $A$  in kJ mole<sup>-1</sup>).

Basing on the very satisfying agreement between the reported measurements of the electrical resistivity in the liquid phase and values obtained from steady-state methods, we think that the exploding wire technique is most capable for the determination of various high temperature properties of metals. The quantitative agreement between the dynamic and the steady-state data is also a convincing indication that the sample is at least close to thermodynamic equilibrium at all times during the heating process. The application of a fast 2-wavelength spectrometer (risetime  $\leq 8$  nsec) for the measurement of the radiation temperature of the heated samples will enable us to determine high-temperature heat capacity. First results of radiation temperature measurements will be reported soon. A better knowledge of the expansion behavior of the liquid metal will improve the method; therefore, we have started a series of experiments which should produce data for the radial and longitudinal expansion of the samples and with that for the correction of the measured resistivities.



- <sup>1</sup> A. Cezairliyan, M. S. Morse, H. A. Berman, and C. W. Beckett, *J. Res. Nat. Bur. Stand.* **74 A**, 65 [1970].
- <sup>2</sup> K. W. Henry, D. R. Stephens, D. J. Steinberg, and E. B. Royce, *Rev. Sci. Instrum.* **43**, 1777 [1972].
- <sup>3</sup> G. R. Gathers, J. W. Shaner, and D. A. Young, *Phys. Rev. Lett.* **33**, 70 [1974].
- <sup>4</sup> M. M. Martynyuk and V. I. Tsapkov, *Ind. Lab.* **40**, 1781 [1974].
- <sup>5</sup> M. M. Martynyuk, I. Karimkhodzhaev, and V. I. Tsapkov, *Sov. Phys.-Tech. Phys.* **19**, 1458 [1975].
- <sup>6</sup> A. I. Savvatimskii, *High Temperature* **11**, 1057 [1975].
- <sup>7</sup> U. Seydel, R. Schöfer, and H. Jäger, *Z. Naturforsch.* **30 a**, 1166 [1975].
- <sup>8</sup> P. W. Bridgman, *Physics of High Pressure*, Bells & Sons, London 1962.
- <sup>9</sup> K. K. Kelley, *Bureau of Mines Bulletin* 584 [1960].
- <sup>10</sup> D. J. Steinberg, *Metall. Trans.* **5**, 1341 [1974].
- <sup>11</sup> M. G. Haines, *Proc. Phys. Soc. London* **74**, 576 [1959].
- <sup>12</sup> U. Seydel, W. Fucke, and B. Möller, *Z. Naturforsch.* **32 a**, 147 [1977].
- <sup>13</sup> R. Hultgreen, R. L. Orr, P. D. Anderson, and K. K. Kelley, *Selected Values of Thermodynamic Properties of Metals and Alloys*, New York-London 1963.
- <sup>14</sup> H.-J. Güntherodt, E. Hauser, H. U. Künzi, and R. Müller, *Phys. Lett.* **54 A**, 291 [1975].
- <sup>15</sup> A. R. Regel and H. P. Mokrinsky, *Zh. Tekh. Fiz.* **28**, 2121 [1953].
- <sup>16</sup> J. Siebke, Thesis, Univ. Kiel, 1974 (to be published).
- <sup>17</sup> W. Kierspe, R. Kohlhaas, and H. Gonska, *Z. Angew. Phys.* **24**, 28 [1967].
- <sup>18</sup> A. Cezairliyan and J. C. McClure, *J. Res. Nat. Bur. Stand.* **78 A**, 1 [1974].